

Article

Artificial Thermal Quenching and Salt Crystallization Weathering Processes for the Assessment of Long-Term Degradation Characteristics of Some Sedimentary Rocks, Egypt

Marzouk Mohamed Aly Abdelhamid ^{1,†}, B. G. Mousa ^{1,†} , Hassan Waqas ² , Mohamed Abdelghany Elkotb ^{3,4} ,
Sayed M. Eldin ⁵ , Iqra Munir ⁶, Rashid Ali ^{7,*}  and Ahmed M. Galal ^{8,9} 

- ¹ Department of Mining and Petroleum Engineering, Faculty of Engineering, Al-Azhar University, Cairo 11884, Egypt
 - ² National Engineering Research Center for Geographic Information System, School of Geography and Information Engineering, China University of Geosciences, Wuhan 430074, China
 - ³ Mechanical Engineering Department, College of Engineering, King Khalid University, Abha 61421, Saudi Arabia
 - ⁴ Mechanical Engineering Department, College of Engineering, Kafrelsheikh University, Kafr El-Sheikh 33516, Egypt
 - ⁵ Center of Research, Faculty of Engineering and Technology, Future University in Egypt, New Cairo 11835, Egypt
 - ⁶ State Key Laboratory of Information Engineering in Surveying, Mapping, and Remote Sensing (LIESMARS), Wuhan University, Wuhan 430079, China
 - ⁷ School of Mathematics and Statistics, Central South University, Changsha 410083, China
 - ⁸ Department of Mechanical Engineering, College of Engineering in Wadi Alddawasir, Prince Sattam bin Abdulaziz University, Wadi Addawaser 11991, Saudi Arabia
 - ⁹ Production Engineering and Mechanical Design Department, Faculty of Engineering, Mansoura University, P.O. Box 35516, Mansoura 35516, Egypt
- * Correspondence: rashidali@csu.edu.cn or rashidali0887@gmail.com
† These authors contributed equally to this manuscript.



Citation: Abdelhamid, M.M.A.; Mousa, B.G.; Waqas, H.; Elkotb, M.A.; Eldin, S.M.; Munir, I.; Ali, R.; Galal, A.M. Artificial Thermal Quenching and Salt Crystallization Weathering Processes for the Assessment of Long-Term Degradation Characteristics of Some Sedimentary Rocks, Egypt. *Minerals* **2022**, *12*, 1393. <https://doi.org/10.3390/min12111393>

Academic Editors: Teresa Pereira da Silva, Daniel P. S. De Oliveira and João Pedro Veiga

Received: 4 September 2022

Accepted: 27 October 2022

Published: 31 October 2022

Publisher's Note: MDPI stays neutral with regard to jurisdictional claims in published maps and institutional affiliations.



Copyright: © 2022 by the authors. Licensee MDPI, Basel, Switzerland. This article is an open access article distributed under the terms and conditions of the Creative Commons Attribution (CC BY) license (<https://creativecommons.org/licenses/by/4.0/>).

Abstract: This research aims at investigating the deterioration of limestone rocks due to the influences of thermal quenching and salt crystallization weathering tests and predicting their long-term durability. Therefore, six types of limestones were quarried from different provinces of Egypt and subjected to 50 cycles of thermal quenching and 25 cycles of salt crystallization weathering processes. The porosity, Schmidt hammer rebound hardness, ultrasound pulse velocity, Brazilian tensile strength, and uniaxial compression strength were determined before and after weathering processes. In addition, the mathematical decay function model was developed to evaluate the degradation rate of samples against weathering processes. Results proved that the cyclic salt crystallization deteriorates the physico-mechanical characteristics of the studied limestone more strongly than the thermal quenching cycles do. The decay constant and half-life indexes obtained here indicate that the degradation rate differs for various limestone specimens under thermal and salt weathering processes. This model also showed that the deterioration rate of the studied rocks was higher during cyclic salt crystallization in comparison with thermal quenching. Therefore, the rock degradation rate and or long-term durability under cyclic thermal and salt processes can be estimated accurately. These results show that the studied limestones can be used as building stones in regions exposed to frequent cyclic thermal and salty weathering conditions for long periods without degradation. However, partial attention should be given to LSG limestone rocks characterized by increased porosity and water absorption characteristics.

Keywords: limestone rocks; thermal quenching; salt crystallization; decay function approach; weathering; long-term degradation

1. Introduction

Natural rocks have been widely used as building and construction stones, especially in historical structures and new engineering applications from the past up to the present times [1–4]. The long-term durability of stones is defined as its resistance to environmental conditions over an extended period of time [5]. Due to the long-term exposure to the atmosphere, rocks are always suffering different recurrent types of weathering processes, resulting in partial or full deterioration [6–9]. Temperature changes are among the major reasons for rock damage in ancient and new engineering structures [10]. All building materials expand when heated and shrink as they cool down. This process is named thermal shock weathering. Thermal quenching is created by sudden changes in temperature and leads to ‘catastrophic’ damage in the form of cracks, so the strength of rock material is suddenly reduced [5].

Many studies have been carried out for investigating the effect of thermal quenching process on the physico-mechanical characteristics of building stones [11–17]. Yavuz et al. [18] performed thermal quenching cycles on carbonate rocks in the laboratory and established a model for predicting the index properties of damaged rocks depending on the initial property and number of thermal quenching cycles. Hale and Shakoor [19] analyzed the variation in the compression strength for sandstone rocks against heating and cooling cycles. Sousa et al. [20] studied the influence of thermal quenching action on granite rocks and found that the compressional wave velocity of granite decreased after thermal quenching test. Wang et al. [21] experimentally studied the influences of thermal shock and freezing–thawing cycles on red sandstone rocks before and after accelerated tests. They indicated an important decrease in the physico-mechanical properties of red sandstone rocks after the thermal shock and freezing–thawing processes. Wang et al. [22] indicated induced change of physico-mechanical characteristics of red sandstone after 10, 20, 30, and 40 thermal quenching cycles. Gokceoglu et al. [23] developed models for estimating the weathering degree of granitic rocks from some parameters, including porosity, ultrasound wave velocity, and unconfined compression strength. Mutluturk et al. [24] established a decay function model for predicting the decrease in rock integrity against heating and cooling. Similarly, salt crystallization is also the most powerful weathering process, especially in marine and mild environmental conditions [25]. Salt crystallization is also one of the significant reasons for the degradation of rocks in nature and in stones used in construction [26]. Crystallization pressure is the most critical damage mechanism during the salt weathering action, which depends mainly on the pore size and super saturation degree [27]. When the crystallization pressure reaches the tensile strength of the rock, new microcracks are developed and the present ones are deepened and widened; thus, this process leads to rock decay [28].

Different studies have been carried out to determine the rock degradation induced by salt crystallization weathering [29–42]. Angeli et al. [43] investigated the impact of temperature and salt concentration on the salt weathering process of a sedimentary rock with sodium sulfate. Cultrone et al. [44] investigated the petro-physical and durability tests on sedimentary rocks to assess their quality as building materials. Vazquez et al. [45] measured the changes in the weight of sedimentary rocks used as building stones against the salt weathering process. Yavuz and Topal [46] studied the impacts of thermal shock and salt crystallization on different types of marble specimens from Western Anatolia, Turkey. Benavente et al. [47] performed laboratory tests on five different kinds of porous stones, concluding that the mechanical characteristics of rocks have a statistically significant weight in the prediction of salt crystallization process, with a small contribution to water transport and pore structure parameters. Yavuz et al. [48] investigated the durability of green andesite rocks through aging weathering processes such as salt crystallization and freezing–thawing cycles. Ruedrich and Siegesmund [49] studied the physical weathering processes under the crystallization of salt and ice in the pores of sandstone rocks. They proved that these pores have a crucial influence on the behavior of rock damage.

Despite the numerous studies conducted on this topic, few lead to the modeling of the alteration phenomenon. Experimental investigations of rocks are essential for the thermal and salt weathering processes, whilst it is also significant to develop damage models and to estimate the degradation rate. Few damage models have been established for evaluating the freezing–thawing and thermal quenching weathering processes [13,22,24,28,50,51], whilst estimating deterioration models against salt crystallization process have not yet reported and there are almost no damage models that take into consideration the mechanical strength properties to evaluate the rock integrity loss due to the cyclic salt crystallization action.

The aims of this research are (1) to better understand the degradation of the selected limestone rock specimens that occurred by the artificial weathering processes, including thermal quenching and salt crystallization, and correlate it with their durability characteristics; (2) to determine their response to the artificial weathering processes through the assessment of their physico-mechanical characteristics described as porosity, Schmidt hammer rebound hardness, ultrasound pulse velocity, and Brazilian tensile and uniaxial compression strengths; and (3) to statistically assess and estimate the long-term durability (integrity decrease rate) of the mechanical strength parameters for limestones against cyclic thermal quenching and salt crystallization by use of a decay function model. In general, this paper contributes to preliminary design stage, engineering structures, replacement works, and safety or stability evolution of rock applications in mild or humid and salty environments.

2. Materials and Methods

2.1. Materials

In this research, six types of limestone rocks were taken out from different localities in Egypt, including South Sinai, Suez, El-Minia, Qena, Sohag, and Aswan (Figure 1). These rocks are used in construction industries. Large blocks were extracted for each rock type ranging in size from 0.3 m × 0.3 m × 0.35 m to 0.35 m × 0.4 m × 0.4 m. Cylindrical and cubical rock samples were obtained in the laboratory for various experiments tests. The tested rock samples were free of any discontinuities or joints to avoid the impact of anisotropy on the measurements. The studied limestone samples were firstly examined under the polarized optical microscope for petrographical analysis using the Eclipse E600POL, based on Nikon’s popular Eclipse E600 microscope, which features a 12-volt, 100-watt internal tungsten halogen illumination system. The microscopic features of the studied limestones are shown in Table 1. The main mineral constituent of all tested specimens is calcite associated with some rare amounts of accessory and or opaque minerals. The chemical analysis was carried out at the Central Laboratories Sector at the Egyptian Mineral Resources Authority, Cairo, Egypt using a ZSX PRIMUS X-ray fluorescence spectrometer (XRF). The ZSX Primus is a 3 or 4 kW WDXRF spectrometer with the thinnest end-window tube (30 microns) and 6 auto-selectable diameters: 35, 30, 20, 10, 1, and 0.5 mm (sample size). The chemical analysis of the studied limestones is presented in Table 2.

Table 1. Petrographic features of the tested limestone rocks.

Rock Type	Code	Locality	Microstructure
Limestone	LSS	South Sinai	Medium-grained calcite texture, oolitic, porous, packstone, cemented, pores filled with rare minerals
Limestone	LSZ	Suez	Fine-grained calcite texture, calcareous massive, slightly porous
Limestone	LEM	El-Minia	Fine-grained calcite texture, slightly hard stone, clastic
Limestone	LQ	Qena	Very fine-grained calcite texture, clastic, compact, marly, hard stone
Limestone	LSG	Sohag	Coarse-grained calcite texture, porous, weak stone
Limestone	LA	Aswan	Medium- to fine-grained calcite texture, semiporous, pack stone

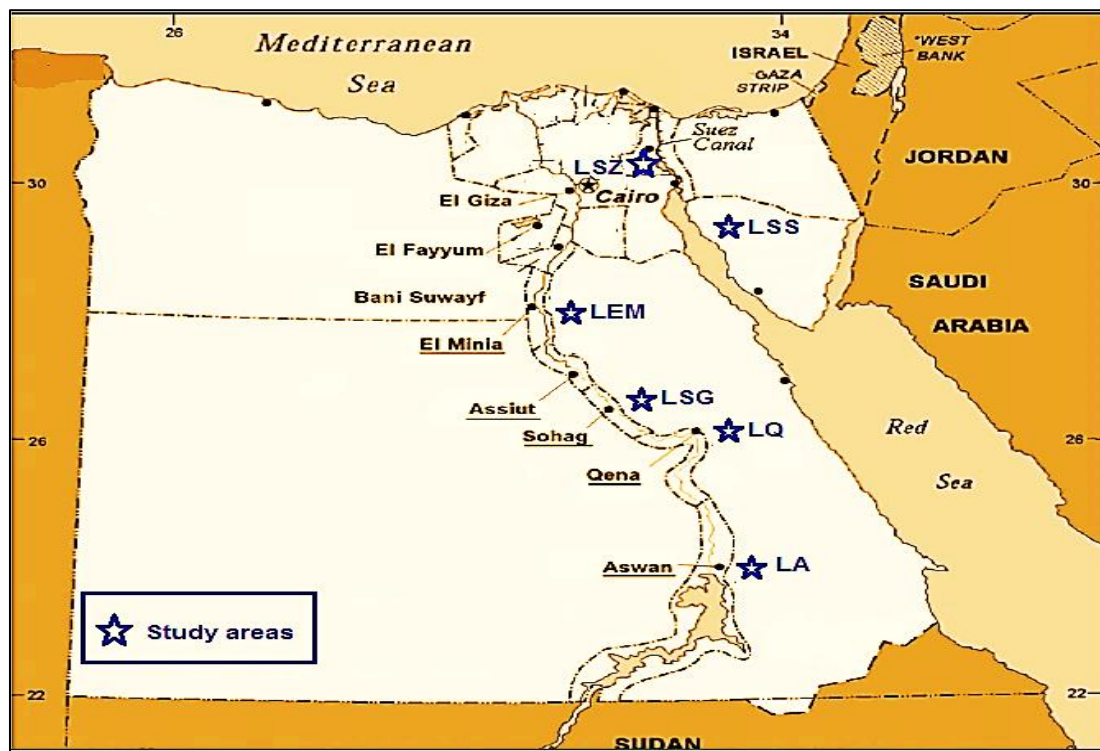


Figure 1. Location map of the studied limestone specimens.

Table 2. XRF analysis of the studied limestones.

Rock type	Locality	CaO	K ₂ O	MgO	Al ₂ O ₃	Na ₂ O	Fe ₂ O ₃	SiO ₂	LOI	Total
LSS	South-Sinai	55.06	0.05	0.30	0.11	0.09	0.15	2.07	42.09	99.92
LSZ	Suez	53.13	0.07	0.60	0.16	0.05	0.17	2.77	43.20	100.15
LEM	El-Minia	51.87	0.04	0.43	0.09	0.04	0.11	3.28	44.25	100.11
LQ	Qena	50.61	0.02	0.33	0.07	0.01	0.10	4.97	43.88	99.99
LSG	Sohag	56.47	0.09	0.66	0.19	0.06	0.23	1.80	40.54	100.04
LA	Aswan	53.39	0.07	0.61	0.15	0.05	0.20	3.78	41.68	99.93
Absolute error (%)		0.030	0.001	0.006	0.002	0.001	0.004	0.013	0.00	

2.2. Methods

Laboratory experiments were carried out for determining the Physico-mechanical properties including, the bulk density, absorption of water, apparent porosity, the compressional wave velocity, the Schmidt hammer rebound hardness, the unconfined compression strength, and the tensile strength (Brazilian). The physical properties, including the density, absorption by weight, and porosity, were determined for rock samples of size (side 5 cm) according to the test methods carried out by TS EN 1936 [52] and TS EN 13755 [53]. Five specimens were tested for each limestone type and their mean values were obtained.

The mechanical properties including the unconfined compression strength and the Brazilian tensile strength were determined. The unconfined compression strength test was carried out on specimens of cubic form (side 10 cm) in accordance with the test methods proposed by ISRM [54] and TS EN 1926 [55]. Five samples were tested for each limestone type and their average values were obtained.

The tensile strength test (Brazilian) was applied in according with the test methods proposed by ISRM [56]. This test was carried out on diametrically shaped samples of 5.0 cm, and the ratio of height to diameter was 0.5. The number of rock samples used in this test was five, and the mean values were taken.

The Schmidt hammer rebound hardness was performed according to the test procedures suggested by ISRM [56] and Aydin [57]. The Schmidt hammer (N-Type) test was carried out on samples of cubic shape (side 10 cm). Twenty individual impacts were performed on each rock specimen. The highest and lowest rebound values were excluded and then the arithmetic mean was taken.

The compressional wave velocity was determined using the ultrasonic system. This test was carried out at the Housing & Building National Research Center (HBRC), Cairo, Egypt. Cylindrical rock specimens with a diameter of 5.0 cm and the ratio of height to diameter of 2.5 were prepared according to the procedures outlined by Martinez-Martinez et al. [58]. The number of tested rock specimens was five, and mean values were determined.

2.3. Artificial Weathering Processes

The thermal quenching weathering test was applied according to EN-14066 [59] recommendations, and salt crystallization was performed in accordance with the general procedures suggested by Rothert et al. [60] for studying the resistance of rock samples to determine the physico-mechanical characteristics and change rates.

2.3.1. Thermal Quenching

A thermal shock weathering test was carried out on specimens of cylindrical shape (5.0 cm). All studied limestone samples were subjected to fifty cycles of thermal quenching weathering. The thermal quenching process consisted of two stages (Figure 2a). Firstly, all limestone specimens were heated in an air-ventilated oven at 70 °C for 18 h. Finally, all specimens were taken out from the oven, and rapidly saturated in distilled water at +20 °C for 6 h. Each thermal shock cycle requires 24 h to be completed. All studied limestone samples were dried to constant weight in an oven at 70 °C before and after cyclic thermal quenching. In this research, two series of limestone rock specimens were prepared; one set of these specimens was used to determine the initial physico-mechanical characteristics before the thermal shock process (unweathered specimens). The second set of specimens was subjected to 10, 20, 30, 40, and 50 cycles, and then the mechanical characteristics, including unconfined compression strength and Brazilian tensile strength, were recorded. Meanwhile, the porosity, the Schmidt hammer rebound hardness, and the ultrasound compressional wave velocity were determined at the end of the 50th cycle.

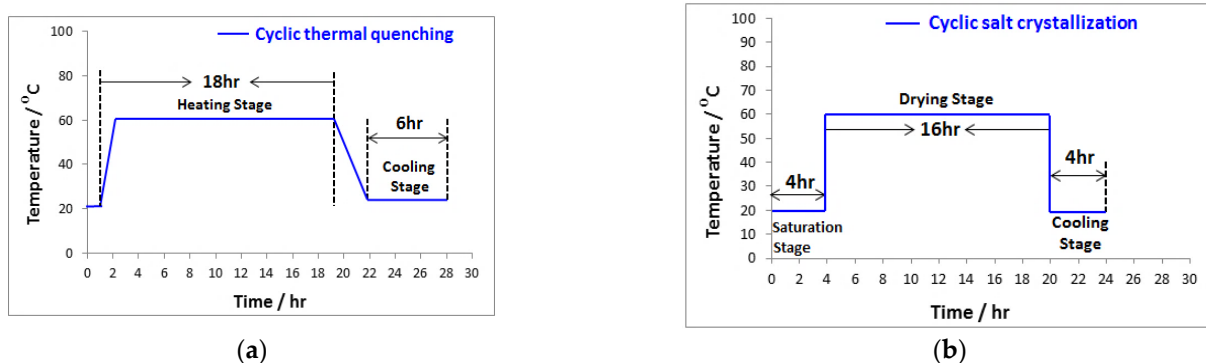


Figure 2. The temperature–time schematic diagram: (a) thermal quenching; (b) salt crystallization.

2.3.2. Salt Crystallization

The salt crystallization weathering process was performed on cubic samples of 5.0 cm by total saturation in a sodium chloride solution (10%). All rock samples were subjected to twenty five cycles of salt crystallization. The salt weathering process consisted of three stages (Figure 2b). Firstly (saturation), the clean and dried rock specimens were placed in a container and saturated in the solution of sodium chloride for a period of 4 h. Secondly (drying), the specimens were taken out from the solution and dried in an air-ventilated oven at 60 °C for 16 h. Thirdly (cooling), the specimens were cooled at room conditions of

20 °C for a period of 4 h. The cycle of the salt crystallization requires 24 h to be completed. In this process, the uniaxial compression strength and the Brazilian tensile strength were carried out at 5, 10, 15, 20 and 25 cycles, whereas the porosity, the Schmidt hammer rebound hardness, and the ultrasound compressional wave velocity were obtained at 25 cycles.

3. Results and Discussions

As studied by many researchers, the long-term deterioration of rocks due to the weathering processes is a function of their physico-mechanical characteristic. Consequently, determination of these properties is significant for the assessment of the stone durability. The mean values of the physico-mechanical properties and standard deviations of the studied limestone rocks before the accelerated weathering processes (fresh samples) are presented in Table 3. This table shows that the average values of dry densities for studied rocks range between 2.44 for the LQ limestone samples and 2.63 for the LSG specimens. The mean values of water absorption of these limestones range between 1.56% (LQ specimens) and 5.5% (LSS samples). The average values of porosity range between 6.89% (LQ samples) and 9.82% (LSS samples). The mechanical strength tests, including uniaxial compression strength and Brazilian tensile strength, were investigated. Table 3 displays the mean values of mechanical strength characteristics of studied rocks. This table indicates the highest uniaxial compression strength of 73.77 MPa for LQ limestone samples in comparison with the lowest (38.08 MPa) for LSS specimens. Similarly, the highest tensile strength of 5.83 MPa was recorded by the LQ limestone samples and the lowest of 3.19 MPa regarding the LSS specimens. A nondestructive test including Schmidt hammer rebound hardness and ultrasonic wave velocity was obtained. The average values of Schmidt rebound hardness range between 30.5 for the LSS limestone samples and 40.7 for the LQ specimens. Moreover, the mean values of ultrasound compressional wave velocity of these rocks range between 3.33 Km/s (LSS limestone samples), and 5.02 Km/s for LQ samples (Table 3). Rock strength is influenced by its pores and voids [61]; hence, permeability, which simplifies the presence of water in the stone, is strongly affected by the value of the porosity [62]. As rock specimens in the current research have porosity <10%, their permeability behavior is determined by their porosity. Consequently, the porosity value is a critical physical parameter that influences the rock characteristics and controls its durability [63]. It is necessary to better understand the correlation between the porosity and the physico-mechanical characteristics of studied rocks. Many studies investigate the relationships between porosity and rock properties. Tuğrul [64] and Diamantis et al. [65] determined relationships between porosity and unconfined compressive strength of rocks. Figure 3 shows the correlation between the porosity and physico-mechanical properties of the studied limestones. Figure 3b–e show an inverse strong linear relationship between porosity and physical and mechanical properties. Therefore, the physico-mechanical characteristics of the tested limestone specimens were influenced by their porosity. However, no important correlation was found between porosity and dry density ($R^2 = 0.0316$) (Figure 3a). Based on these results, the physico-mechanical properties of the studied limestone rocks decrease with increased porosity. Figure 4 displays a three-dimensional view of the effect of porosity (n) on the Schmidt rebound hardness (SCH), ultrasound pulse velocity (UPV), tensile strength (TS), and uniaxial compression strength (UCS) for the tested limestone rocks.

Table 3. Average values of the physico-mechanical properties and standard deviations of fresh specimens.

Rock Type	ρ_d (g/cm ³)		W (%)		n (%)		SCH		UPV (Km/s)		Ts (MPa)		UCS (MPa)	
	Mean	SD	Mean	SD	Mean	SD	Mean	SD	Mean	SD	Mean	SD	Mean	SD
LSS	2.46	0.08	5.50	0.64	9.82	0.95	30.5	1.65	3.33	0.39	3.19	0.37	38.08	1.74
LSZ	2.61	0.11	2.26	0.41	7.99	1.17	36.9	0.99	4.67	0.65	5.15	0.62	54.95	1.71
LEM	2.49	0.07	1.61	0.44	7.47	0.83	38.3	1.06	4.81	0.44	5.42	0.72	66.90	1.75

Table 3. Cont.

Rock Type	ρ_d (g/cm ³)		W (%)		n (%)		SCH		UPV (Km/s)		Ts (MPa)		UCS (MPa)	
	Mean	SD	Mean	SD	Mean	SD	Mean	SD	Mean	SD	Mean	SD	Mean	SD
LQ	2.44	0.09	1.56	0.38	6.89	0.90	40.7	1.41	5.02	0.53	5.83	0.99	73.77	1.65
LSG	2.63	0.10	4.80	0.40	9.33	0.72	33.8	1.18	3.78	0.88	3.99	0.65	41.05	2.36
LA	2.52	0.06	4.30	0.52	8.80	0.91	35.4	1.13	4.02	0.75	4.19	0.60	45.97	2.02
No of tested specimens	5		5		5		5		5		5		5	

(ρ_b) Dry density, (W) water absorption, (n) porosity, (SCH) Schmidt hammer rebound hardness, (UPV) ultrasound compressional pulse velocity, (Ts) Tensile strength, and (UCS) uniaxial compression strength. LSS (Limestone—South-Sinai), LSZ (Limestone—Suez), LEM (Limestone—El-Minia), LQ (Limestone—Qena), LSG (Limestone—Sohag), and LA (Limestone—Aswan).

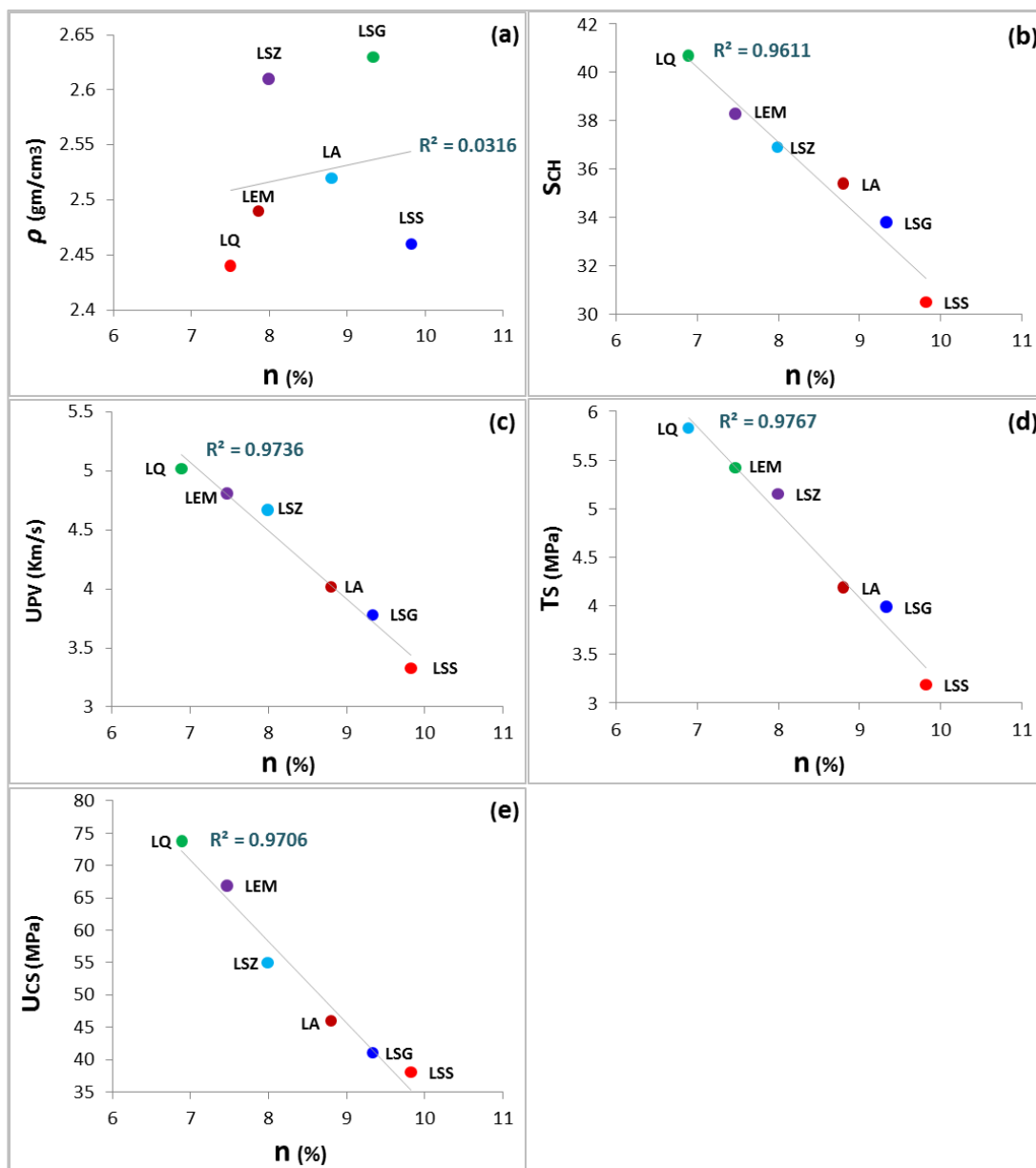


Figure 3. Relationship between porosity, n (%) and (a) density, ρ (g/cm³), (b) Shmidt hammer rebound, SCH, (c) ultra sound pulse velocity, UPV (Km/s), (d) tensile strength, Ts (MPa), and (e) uniaxial compression strength, UCS (MPa).

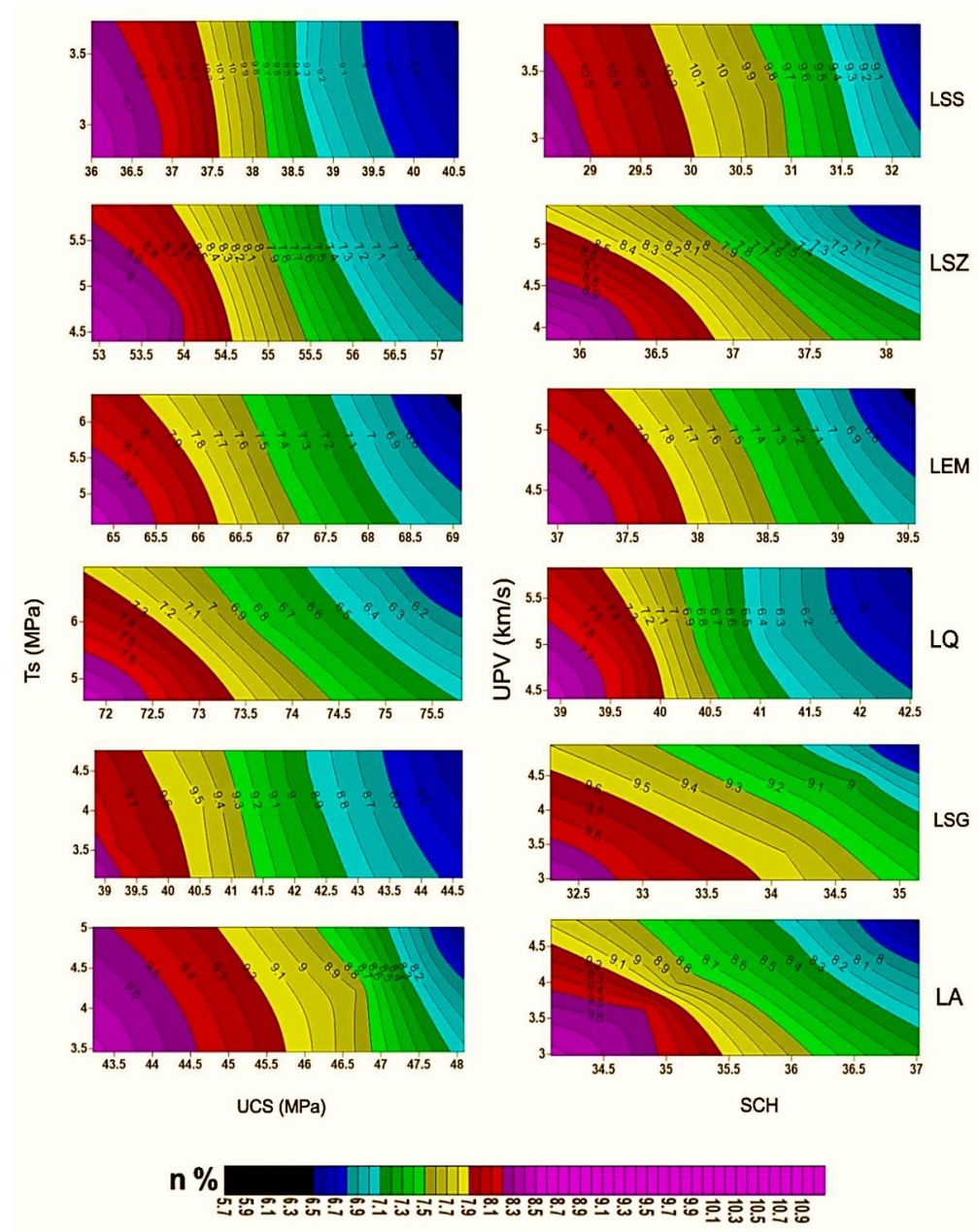


Figure 4. Influence of porosity (n) on TS, UCS, UPV, and SCH for the tested limestone specimens.

3.1. Influence of Cyclic Thermal Quenching Weathering on Physicomechanical Characteristics

Table 4 shows the assessment of the physico-mechanical characteristics before and after cycles of thermal quenching weathering. The porosity, Schmidt hammer rebound hardness, and ultrasound pulse velocity are determined at the end of 50 cycles. Meanwhile, the tensile strength and uniaxial compression strength are determined at 10, 20, 30, 40 and 50 cycles, and then their mean values and standard deviations are presented in Table 4. Generally, the tested limestone specimens did not indicate an important visual degradation after the thermal quenching weathering process. There were no visible granular disintegrations and edge fissures in the tested rock specimens after thermal quenching cycles. As can be seen in Table 4, the results show that the porosity values increase for the tested rock specimens with the number of thermal quenching cycles, whereas the Schmidt hammer rebound hardness, ultrasound pulse velocity, Brazilian tensile strength, and uniaxial compression strength decrease. As seen in this table, after the end of the 50 cycles, the LSG limestone samples exhibit the highest increase in porosity value, while the lowest was for LQ specimens.

Table 4. Mean values and standard deviations of the physico-mechanical properties under cyclic thermal quenching.

Cyclic Number	LSS		LSZ		LEM		LQ		LSG		LA	
	Mean	SD										
n (%)												
0	9.82	0.95	7.99	1.17	7.47	0.83	6.89	0.90	9.33	0.72	8.80	0.91
50	9.94	0.99	8.14	1.12	7.55	0.95	6.95	0.99	9.51	0.66	8.97	1.07
SCH												
0	30.51	1.65	36.90	0.99	38.44	1.06	40.71	1.41	33.8	1.18	35.4	1.13
50	29.11	1.09	35.05	1.11	37.10	1.27	39.70	1.33	31.9	1.29	33.7	1.28
UPV (Km/s)												
0	3.23	0.39	4.67	0.65	4.81	0.44	5.02	0.53	3.78	0.88	4.02	0.75
50	3.10	0.44	4.53	0.77	4.70	0.62	4.95	0.50	3.56	1.04	3.82	0.80
Ts (MPa)												
0	3.19	0.37	5.15	0.72	5.42	0.62	5.83	0.99	3.99	0.65	4.19	0.60
10	2.95	0.39	5.03	0.77	5.26	0.78	5.75	1.10	3.65	0.66	3.98	0.50
20	2.83	0.28	4.83	0.80	5.10	0.80	5.69	1.04	3.40	0.70	3.57	0.67
30	2.56	0.44	4.55	0.96	4.99	0.77	5.55	0.90	3.12	0.98	3.33	0.89
40	2.35	0.50	4.28	0.91	4.72	0.84	5.33	0.95	2.75	0.91	2.88	0.70
50	2.30	0.45	3.80	0.76	4.41	0.93	5.07	0.87	2.25	0.84	2.59	0.99
UCS (MPa)												
0	38.08	1.74	54.95	1.71	66.90	1.75	73.77	1.65	41.05	2.32	45.97	2.02
10	36.55	2.10	51.15	1.66	65.11	2.12	73.02	1.59	37.36	2.55	41.57	2.22
20	33.82	2.04	47.10	1.77	63.50	1.80	71.89	1.87	34.56	2.23	36.54	2.43
30	31.75	1.99	45.15	2.05	60.14	1.98	69.18	2.14	31.23	2.67	33.70	2.30
40	28.65	1.67	42.98	1.99	56.84	1.95	66.65	2.23	26.66	2.11	30.54	2.25
50	27.83	1.89	41.29	1.85	55.9	2.02	65.99	1.77	25.00	1.99	29.32	2.61

The main reason for degradation in the thermal shock process is the difference in the thermal shrinkage and contraction of the inside and outside area of the mineralogical composition of the samples [15]. Heating water in the micro-fractures during the thermal shock test reduces the rock structure through moving the soluble minerals toward the stone surface [19]. Therefore, changes in the porosity value related to variations in mineralogical and chemical composition, especially the percentage of calcite, which has a higher tendency to shrinkage and contract than other minerals. It can also be seen that after 50 cycles, the LQ limestone specimens show the lowest decrease in the Schmidt hammer rebound, while the highest was for LSG samples. Table 4 also shows that after 50 cycles, the LSG and LA limestone samples exhibit the highest reduction in ultrasound pulse velocity, while the lowest was for the LQ and LEM specimens. This is due to the thermal quenching process producing new internal cracks that lead to a decrease in ultrasound wave velocity. Therefore, it can be said that the studied limestone specimens, namely LQ and LEM, are less sensitive to the devastating influence of thermal quenching.

Generally, it can be concluded that the change in porosity values for the studied limestones is less sensitive to the influence of cyclic thermal quenching compared to the Schmidt hammer rebound and ultrasound wave velocity values. Figure 5 shows a three-dimensional view of the influence of the number of thermal quenching cycles on the tensile strength and uniaxial compression strength for the tested limestones. This figure shows that an increase in the thermal quenching cycles decreased Brazilian tensile strength and uniaxial compression strength values.

Table 4 and Figure 5 show that after 50 cycles, the LSG limestone samples have the lowest values of Brazilian tensile strength and uniaxial compression strength, while the highest values were for LQ specimens. Due to the cyclic thermal quenching, the loss of tensile strength and unconfined compression strength are related to porosity and/or micro-fissures. Therefore, these specimens were more affected than those LQ specimens due to having the

highest increase in porosity. Overall, it is concluded that the limestone specimens, namely LQ and LEM, exhibited the highest durability under the influence of thermal quenching cycles, whilst the lowest durability was for the LSG and LA rock specimens.

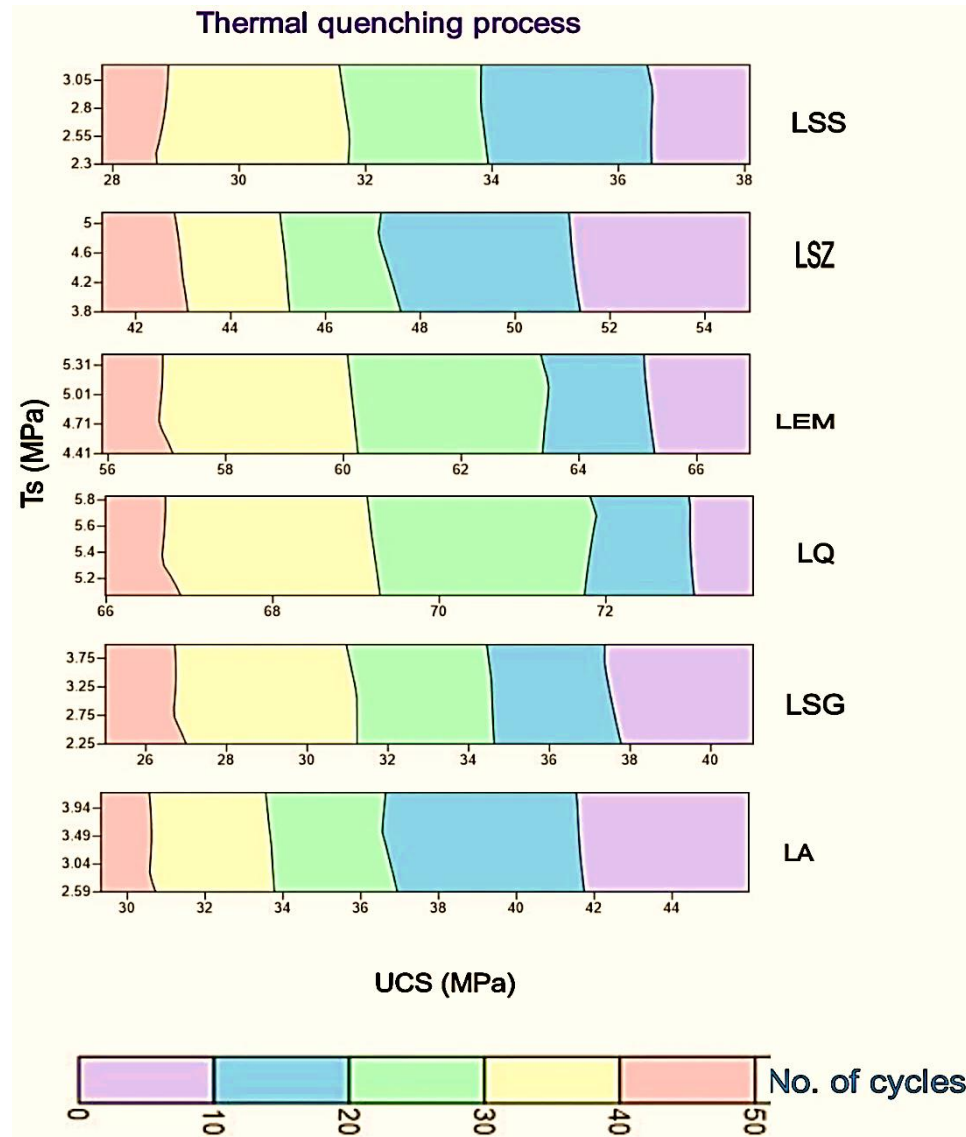


Figure 5. Relationship between TS and UCS values and number of thermal quenching cycles.

3.2. Influence of Cyclic Salt Crystallization Weathering on Physicomechanical Properties

Table 5 presents the mean values of the physico-mechanical characteristics before and after the salt crystallization cycles. The porosity, Schmidt hammer rebound hardness, and ultrasound pulse velocity were determined after the end of 25 cycles. The tensile strength and uniaxial compression strength were determined at 5, 10, 15, 20 and 25 cycles, and then their average values and standard deviations are displayed in Table 5. As seen in this table, the results show that the porosity values increased with the number of salt crystallization cycles, whilst the Schmidt rebound hardness, ultrasound pulse velocity, Brazilian tensile strength, and uniaxial compressive strength decreased. As observed in this table, at the end of 25 cycles, the LSG limestone specimens showed the highest increase in porosity, while the lowest was for LQ samples. The changes in porosity values under salt crystallization are linked to the variations in the size of the pores size within the rock specimens. Therefore, different degradations may occur.

Table 5. Average values and standard deviations of physico-mechanical properties due to salt crystallization cycles.

Cyclic Number	LSS		LSZ		LEM		LQ		LSG		LA	
	Mean	SD										
n (%)												
0	9.82	0.95	7.99	1.17	7.47	0.83	6.89	0.90	9.33	0.72	8.80	0.91
25	10.03	1.11	8.24	1.30	7.67	0.90	7.05	1.04	9.64	1.0	9.08	1.20
SCH												
0	30.51	1.65	36.90	0.99	38.44	1.06	40.71	1.41	33.80	1.18	35.43	1.13
25	28.00	1.77	33.80	1.09	36.60	1.13	39.34	1.47	30.20	1.11	32.10	1.29
UPV (Km/s)												
0	3.23	0.39	4.67	0.65	4.81	0.44	5.02	0.53	3.78	0.88	4.02	0.75
25	3.02	0.49	4.44	0.73	4.62	0.55	4.86	0.76	3.48	0.97	3.76	0.66
Ts (MPa)												
0	3.19	0.37	5.15	0.72	5.42	0.62	5.83	0.99	3.99	0.65	4.19	0.60
5	2.94	0.44	4.90	0.88	5.18	0.85	5.74	1.02	3.55	0.87	3.86	0.65
10	2.77	0.50	4.65	0.90	5.01	0.90	5.63	1.11	3.25	0.73	3.29	0.75
15	2.41	0.41	4.26	0.88	4.88	0.80	5.40	0.92	2.95	0.90	2.99	0.78
20	42.17	0.70	3.90	1.05	4.56	0.66	5.29	0.96	2.45	0.88	2.62	0.59
25	2.03	0.66	3.35	1.11	4.30	0.78	4.95	0.77	1.86	1.10	2.25	0.81
UCS (MPa)												
0	38.08	1.74	54.95	1.71	66.90	1.75	73.77	1.65	41.05	2.32	45.97	2.02
5	35.90	2.27	49.85	1.89	64.55	2.14	72.12	1.70	35.16	2.40	39.88	2.16
10	32.99	2.14	46.12	1.75	61.88	1.99	70.79	1.94	30.66	2.15	34.12	2.22
15	30.15	1.90	43.55	2.22	59.24	1.86	68.22	2.01	27.67	2.60	31.07	2.07
20	27.12	1.99	39.58	1.80	56.77	1.90	65.25	2.10	23.02	2.43	27.89	2.28
25	24.65	2.18	37.12	1.99	54.02	2.22	63.98	1.99	21.22	2.70	26.64	2.35

Based on the degree of disintegration, the development of minute fissures at the corners and surfaces was observed in the LSG specimens after the salt crystallization cycles. Similarly, the LSG limestone samples had the highest decrease in Schmidt rebound hardness, while the lowest was for the LQ specimens. As also seen in Table 5, at the end of 25 cycles, the LSG limestone specimens had the highest decrease in ultrasound pulse velocity, while the lowest was for LQ samples. The compressional wave velocity depends on porosity, pore space, strength, and degree of disintegration [66]. The micro-fissures and pores are the most crucial parameters for decreasing the ultrasound wave velocity. This is evident in LSG limestone specimens. Therefore, it can be said that the loss of ultrasound wave velocity for limestone specimens after the salt crystallization cycles is related to the dilation and enlargement of pores and fractures. Figure 6 presents a three-dimensional view of the effect of the number of salt crystallization cycles on the tensile and uniaxial compression strengths for the studied limestones. As seen in this Figure, the progression of the number of salt crystallization cycles caused a reduction in the values of Brazilian tensile strength and uniaxial compression strength. Table 5 and Figure 6 show that after 25 cycles, the LSG limestone specimens had the lowest values of uniaxial compression and Brazilian tensile strengths, while the highest values were for LQ samples.

It is said that the variation of tensile strength and unconfined compressive strength values is due to the widening and dilation of pre-existing micropores during the salt crystallization process affecting the mechanical behavior of limestone specimens [15].

Previous studies proved that porosity and water absorption are the most significant parameters affecting the behavior of rocks and durability control against the salt weathering test [63]. Therefore, it can be believed that the limestone rocks with the highest increase in porosity will be subject to a high level of disintegration and result in lower durability compared to rocks with the lowest increase in porosity. Therefore, it is said that the

limestone rock samples, namely LSG, exhibited the highest level of degradation against the salt crystallization weathering cycles, whereas the lowest level of deterioration was for LQ rock samples. The major reason for such disintegration of the physico-mechanical parameters against the cyclic salt crystallization process is the high pressure caused by precipitation of salt crystals within the pores and discontinuities of rock specimens. Hence, new microcracks were developed, and finally, the rock was damaged [67].

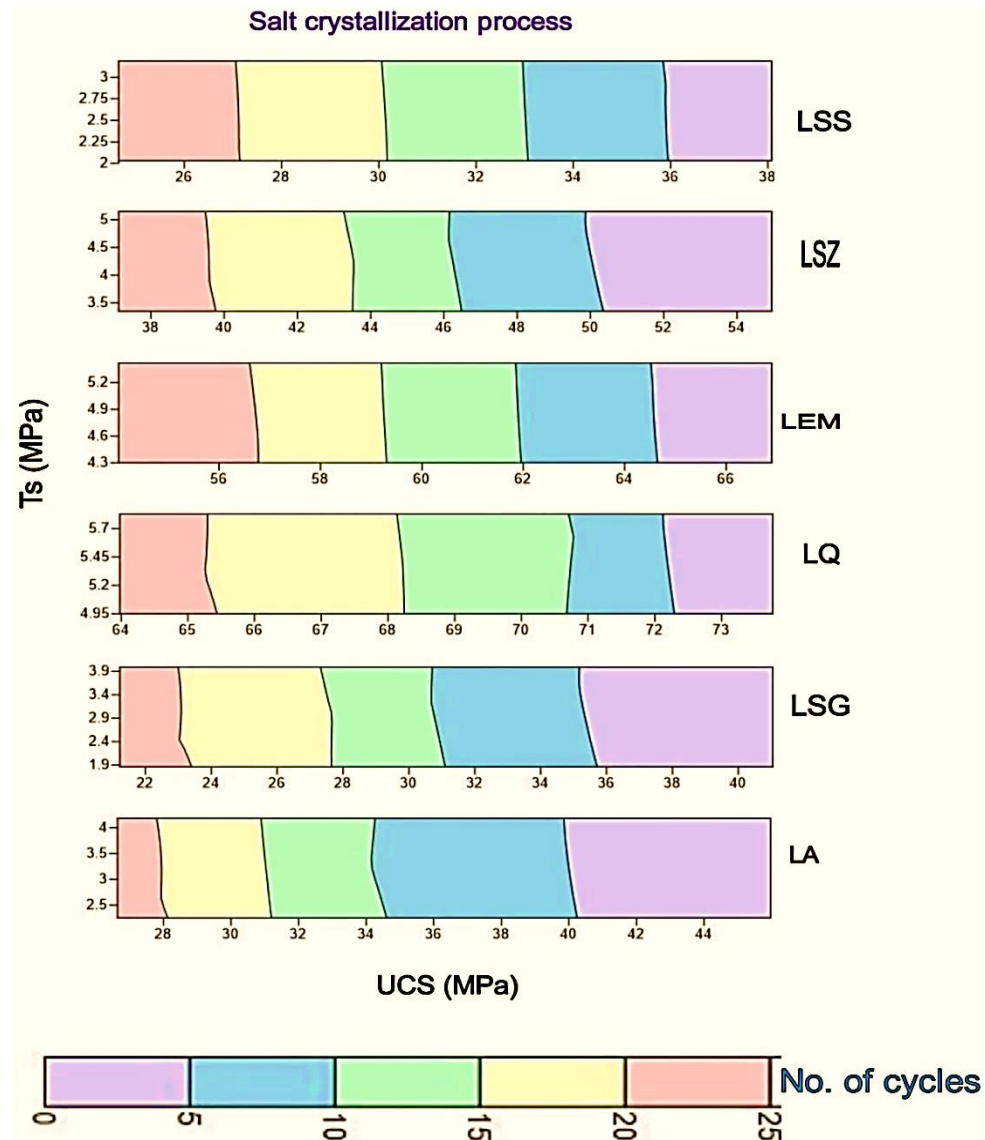


Figure 6. Relationships between TS and UCS values and number of salt crystallization cycles.

The results show that the limestone samples of LSG have the lowest durability against the salt crystallization cycles due to having the highest reduction in the values of tensile strength and uniaxial compression strength, whereas the LQ and LEM rocks have the lowest decrease concerning these properties (Figure 6).

Overall, it is concluded that the change of physico-mechanical properties of the studied limestone rocks is more sensitive to the destructive influences of cyclic salt crystallization weathering than the thermal quenching process.

Brazilian tensile strength and uniaxial compression strength are the most sensitive parameters against the influences of thermal quenching and salt crystallization weathering tests, so their rates of variation are obtained after the end of every ten cycles of the thermal process and after the end of every five cycles of the salt weathering process. The variation

rate determines the degree of rock material deterioration. Figure 7 shows the relationship between the change rate of tensile and uniaxial compression strengths (ΔTS % and ΔUCS %) against the cyclic thermal quenching and salt crystallization weathering processes. As seen in Figure 7, after the end of the cyclic weathering processes, there was a high decrease in the change rate of tensile strength and uniaxial compression strength for limestone samples, namely LSG, while LQ specimens showed the lowest decrease compared to other rocks.

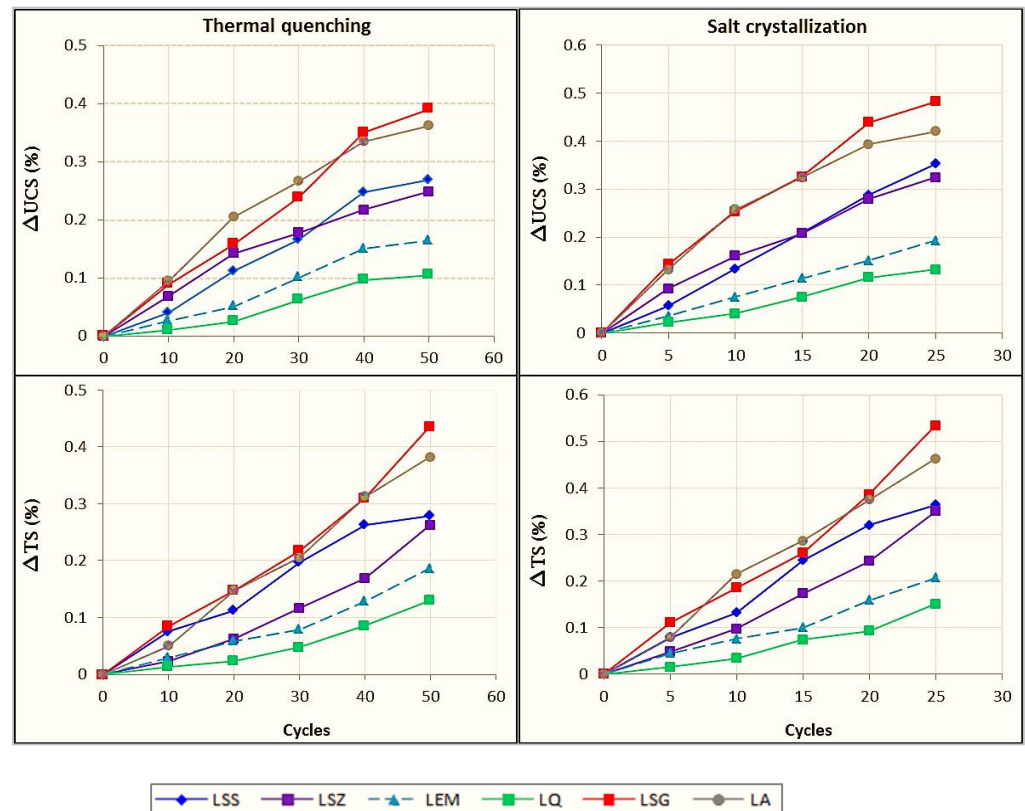


Figure 7. Change rate of TS and UCS values due to the cyclic thermal quenching and salt crystallization.

As this Figure shows, after the end of 50 cycles of thermal quenching, the highest percentage decreases in uniaxial compression strength and tensile strength were 39.1% and 43.6%, respectively, for LSG limestone specimens, whilst the lowest percent reduction was for LQ samples (10.5% and 13%, respectively). Similarly, for the salt crystallization process, it is seen that after the end of 25 cycles, the highest percentage decreases in uniaxial compression strength and tensile strength were 48.3% and 53.4%, respectively, for LSG limestone specimens, whereas the lowest percent decrease was for LQ samples (13.3% and 15.1%, respectively). Therefore, it is observed that limestone rocks, namely LSG have low durability under the influence of accelerated weathering processes compared to other rocks, whereas limestone rocks, namely LQ and LEM, have the highest resistance and durability to the effect of weathering processes. Based on these results, it is concluded that the studied limestone rock specimens are more sensitive to the destructive effect of the salt crystallization process than the thermal quenching. In general, it is said that the change limits of the data obtained for the LSG and LA limestone samples are high, so these types cannot withstand cyclic weathering processes compared to other rocks. Therefore, these stones may not be suitable for construction purposes in humid and salty environments.

3.3. Degradation Model of the Mechanical Strength Parameters

Thermal quenching and salt crystallization weathering processes in the lab are significant for obtaining the necessary data on rock decay, yet insufficient to assess the long-term deterioration.

Mutlutürk et al. [24] postulated the decay function model by using a decay constant (λ) and half-life ($N_{1/2}$) parameters as Equation (1) to express the degradation rate of rock under cyclic freeze–thaw and heat–cool weathering tests, which could also be expressed in an exponential model as Equation (2) by integrating Equation (1) between the initial integrity (I_0) and the integrity after N cycles (I_N). To determine the long-term durability of rock, the decay constant (λ) indicates the mean relative decrease in rock integrity by the work of any single cycle, and the half-life ($N_{1/2}$) refers to the number of cycles required to decrease the rock integrity to its half-value, which is obtained as Equation (3) by replacing ($I_0/2$) with I_N in Equation (2):

$$-(dI/dN) = \lambda N \quad (1)$$

$$I_N = I_0 e^{-\lambda N} \quad (2)$$

$$N_{1/2} = 0.6930/\lambda \quad (3)$$

where $e^{-\lambda N}$ is the decay factor, which shows the proportion of the remaining integrity after number of cycles, i.e., (I_N / I_0); I is the rock integrity; N is the number of cycles; (dI/dN) is the standard for the degradation rate. The model postulated by Mutlutürk et al. [24] considered only the physical parameters, and other mechanical properties were ignored. Therefore, in our study, for investigating the model validity and evaluating the model parameters, laboratory tests of Brazilian tensile strength and uniaxial compression strength of limestone rocks for predicting the integrity decrease rate due to cyclic thermal quenching and salt crystallization were performed. A simple regression analysis method was used to determine the decay constant (λ). According to the model, the data obtained from the laboratory investigations of tensile strength and uniaxial compression strength were exponentially fitted. The degree of fit to this model (curve) can be measured by the value of determination coefficients (R^2), which measure the proportion of variation in the dependent variable [68]. The high values of the determination coefficients indicate that the proposed model fits the data well and facilitates the prediction of the rock sample's properties after any cycle of artificial weathering processes. The fitted curves and experimental data results of tensile strength and uniaxial compression strength for the different limestone rocks against cyclic thermal quenching and salt crystallization weathering processes are illustrated in Figure 8. Based on the previously mentioned experimental results of the Brazilian tensile strength and uniaxial compression strength for the limestone rock types against the cyclic thermal quenching and salt crystallization (Tables 4 and 5), the values of the decay constant (λ) are determined graphically in Figure 8 and listed in Tables 6 and 7; in addition, the half-life ($N_{1/2}$) values obtained from Equation (3) are detailed in Tables 6 and 7.

3.3.1. Decay Constant (λ)

Figure 8 and Tables 6 and 7 show the decay constant values and the determination coefficients (R^2) obtained from the results of mechanical strength parameters, including Brazilian tensile strength (T_s , MPa) and uniaxial compression strength (UCS, MPa) of the studied limestone rocks due to the effect of thermal quenching and salt crystallization cycles. As seen in Figure 8, the integrity loss of the uniaxial compression strength and tensile strength show relatively high values of the decay constant and a rapid integrity decrease rate (rapid durability rate) of the studied rocks, especially in the salt crystallization process. It can also be seen that the high values of the determination coefficients indicate that the proposed model fits the data well and is reliable for predicting the loss of mechanical strength parameters and/or long-term durability of the studied limestone rock specimens after any thermal quenching and/or salt crystallization cycle.

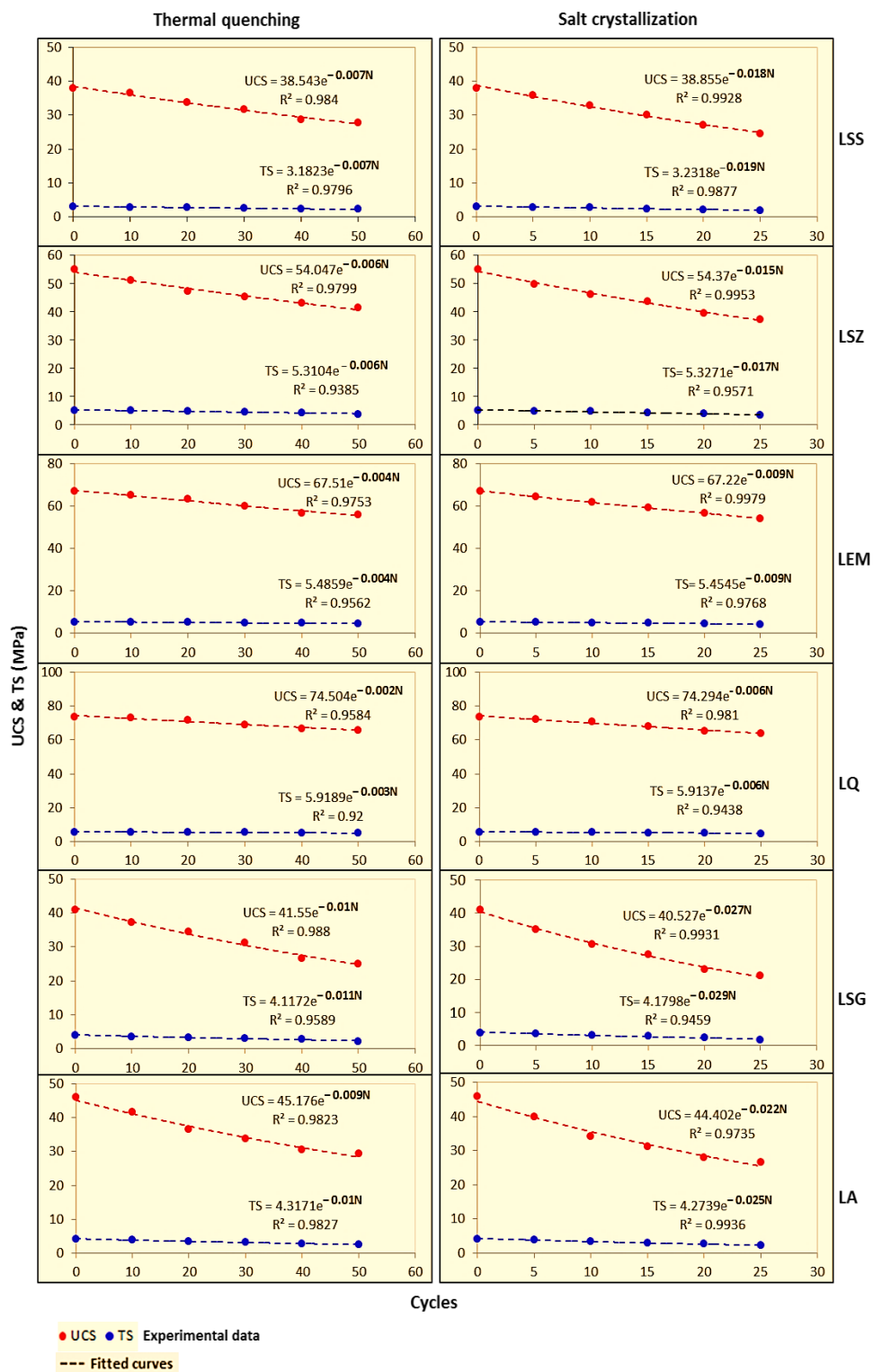


Figure 8. Determining decay constant (λ) based on TS and UCS data against cyclic thermal and salt weathering.

Table 6. Decay constant (λ), half-life ($N_{1/2}$), and coefficient of determination (R^2) of tensile strength parameter due to cyclic thermal shock and salt crystallization.

	Tensile Strength TS (MPa)					
	Thermal Quenching			Salt Crystallization		
	λ	$N_{1/2}$	R^2	λ	$N_{1/2}$	R^2
LSS	−0.007	99.0	0.9796	−0.019	36.5	0.9877
LSZ	−0.006	115.5	0.9385	−0.017	40.8	0.9571
LEM	−0.004	173.3	0.9562	−0.009	77.0	0.9768
LQ	−0.003	231.0	0.9200	−0.006	115.5	0.9438
LSG	−0.011	63.0	0.9589	−0.029	23.9	0.9459
LA	−0.010	69.3	0.9827	−0.025	27.7	0.9936

Table 7. Decay constant (λ), half-life ($N_{1/2}$), and coefficient of determination (R^2) of uniaxial compression strength parameter due to cyclic thermal shock and salt crystallization.

	Uniaxial Compression Strength UCS (MPa).					
	Thermal Quenching			Salt Crystallization		
	λ	$N_{1/2}$	R^2	λ	$N_{1/2}$	R^2
LSS	−0.007	99	0.9840	−0.018	38.5	0.9928
LSZ	−0.006	115.5	0.9799	−0.015	46.2	0.9953
LEM	−0.004	173.3	0.9753	−0.009	77	0.9979
LQ	−0.002	346.5	0.9584	−0.006	115.5	0.981
LSG	−0.010	69.3	0.9880	−0.027	25.7	0.9931
LA	−0.009	77.0	0.9823	−0.022	31.5	0.9735

It is concluded that the sedimentary rocks of the same kind provide good information about their long-term deterioration against the impact of cyclic weathering processes. For example, as seen in Table 6, one of the highest durable limestone samples (LQ) and also one of the least durable specimens (LSG), due to the influence of thermal quenching process (i.e., showing the lowest and highest decay constant values, ($\lambda = -0.003$ and -0.011 , respectively), are of the same rock type. In fact, the tensile strength value of the LQ specimens decreased by 0.3% compared to their initial value, on average, after one thermal quenching cycle, whereas the LSG specimens decreased by 1.1%. Therefore, the integrity decrease rate (degradation rate) of LSG limestone specimens is 3.7 times more than that of the LQ specimens. Similarly, for the cyclic salt crystallization, some of the highest durable samples (LQ) and the least durable specimens (LSG) (i.e., exhibiting the lowest and highest decay constant, ($\lambda = -0.006$ and -0.029 , respectively). Indeed, the LQ specimens lost only 0.6% of their main tensile strength value, on average, after one cycle of salt crystallization, while the LSG specimens decreased by 2.9%. As a result, the integrity loss rate of the LSG specimens is 4.8 times more than that of the LQ specimens (Table 6). Therefore, according to the presented results in Tables 6 and 7, it can be said that the studied limestone specimens exposed to the salt crystallization cycles exhibited the highest values of the decay constant compared to the thermal quenching process.

3.3.2. Half-Life ($N_{1/2}$)

The values of the half-life ($N_{1/2}$) of the loss of tensile and uniaxial compressive strengths of the studied limestones due to the cyclic thermal quenching and salt crystallization are also listed in Tables 6 and 7 and graphically illustrated in Figures 9 and 10, respectively. Based on the results of the tensile strength under the cyclic thermal quenching presented in Table 6 and Figure 9, the limestone specimens, namely LQ, have the longest half-life (231 cycles), whilst the LSG samples have the shortest half-life (63 cycles). For the cyclic salt crystallization, it can also be seen that the LQ samples exhibit the longest half-life (115.5 cycles), while the shortest half-life is for LSG specimens (23.9 cycles). Similarly, according to the data of the uniaxial compression strength against the cyclic thermal quench-

ing listed in Table 7 and Figure 10, the LQ limestone samples show the longest half-life (346.5 cycles), whilst the LSG specimens have the shortest half-life (69.3 cycles). For the salt crystallization process, it can also be seen that the LQ samples exhibit the longest half-life (115.5 cycles), while the shortest half-life is for LSG specimens (25.9 cycles). As shown in Figures 9 and 10, the half-life values based on the tensile strength and uniaxial compression strength parameters, respectively, are similar in some of the studied limestone specimens. The half-life values have no meaningful pattern with respect to the rock kind. Actually, rocks linked to the same origin can indicate a clear variation in long-term deterioration due to the various weathering processes in some cases. Therefore, the type of rock alone cannot provide sufficiently useful information related to the durability of rock specimens under the artificial weathering processes. Eren and Bahali [69] measured the reduction in weight of two different types of limestone under cyclic freezing–thawing. They noticed that the rocks regarding the same origin could indicate clearly different behaviors under freezing–thawing action, and this is due to change in their porosity. Mutluturk et al. [24] measured the shore hardness changes of some various rock types against freezing–thawing cycles. They showed that the rock type alone does not give a clue for the half-life of rocks due to cyclic freezing–thawing.

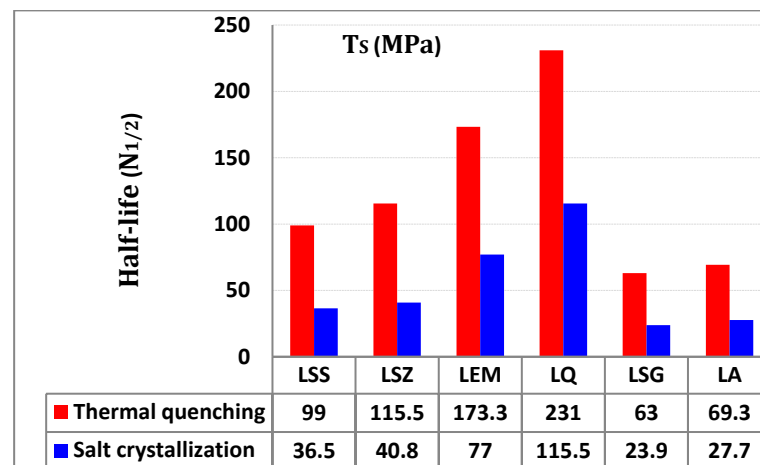


Figure 9. Half-life values of tensile strength of limestones under cyclic thermal and salt weathering.

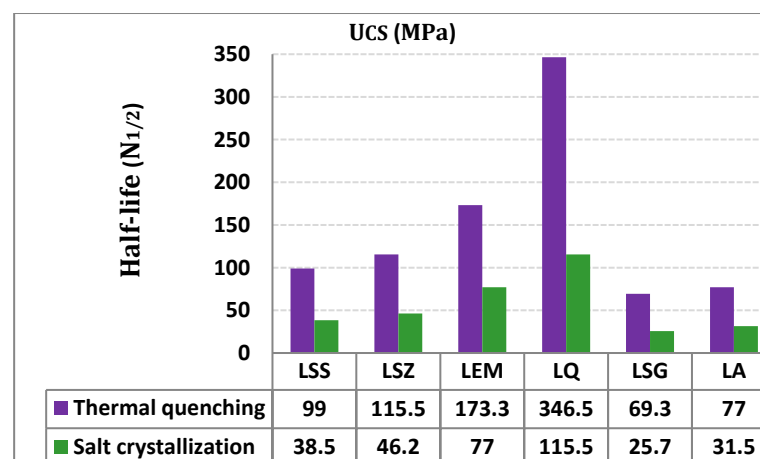


Figure 10. Half-life values of uniaxial compression strength of limestones under the thermal and salt weathering.

According to the current results, it is seen that the half-life values of the integrity loss of the strength properties (Ts and UCS) for the studied limestone rock specimens due to the impact of salt crystallization cycles are lower than those the thermal quenching process.

Overall, it can be concluded that studied limestones were more sensitive to deterioration under the salt crystallization process than thermal quenching.

4. Conclusions

Rock deterioration subject to various physical weathering conditions was assessed by performing the laboratory's cyclic thermal quenching and salt crystallization tests and using the decay function model parameters (decay constant and half-life) to provide helpful information for the assessment of their durability. In addition, the studied limestone rock specimens were also subjected to a series of laboratory experimental tests for determining their physico-mechanical characteristics. In this study, the cyclic thermal quenching and salt crystallization weathering processes were carried out on six different limestone types used for construction purposes in Egypt to evaluate their long-term degradation. In general, the present results show the strong impact of salt crystallization cycles on the rock physico-mechanical characteristics compared to thermal quenching. Therefore, the major following findings can be drawn from the current work:

1. The studied limestone rocks are more sensitive to the destructive effect of the salt crystallization action than the thermal quenching weathering process. The tested limestone rock samples, namely LSG, showed the most significant increase in porosity (3.30%) and the highest percentage decrease in uniaxial compression strength and tensile strength (48.3% and 53.4%), respectively, after the cyclic salt crystallization compared to the other limestone samples. Therefore, the thermal quenching process is not very destructive to the tested limestone samples with high strength and durability compared to salt crystallization. After the end of the cyclic salt crystallization, a slight disintegration was observed at the edges and corners of the LSG samples. Therefore, the studied limestone samples can be used as building stones in mild or humid and salty areas for a long time without degradation. Nevertheless, partial attention must be given to the LSG limestone type.
2. The lowest deterioration level was recorded for the LQ rock samples due to their low porosity and water absorption capacity. Therefore, these specimens were more resistant to weathering processes than other samples.
3. The tested rock specimens under cyclic thermal quenching showed low variations in their physico-mechanical properties. The major reason for these changes is the presence of calcite mineral that leads to anisotropic pressures. These pressures may reopen micro-fractures or pores and finally damage the rock. Overall, the cyclic salt weathering process deteriorated the physical and mechanical characteristics of the rock samples compared to the thermal quenching action.
4. An exponential decay model is applied for predicting the integrity loss characteristics (disintegration rate) of the mechanical strength properties for the tested limestones following cyclic thermal quenching and salt crystallization weathering. This model exhibited a higher sensitivity of limestone rock samples to the cyclic salt weathering process. High values of the decay constant were attained under salt crystallization weathering in comparison with the thermal quenching action, so this model is capable of predicting the degradation rate (integrity loss) of limestone rock specimens without performing any testing and is appropriate for rocks quarried from the same type.

After investigating the artificial weathering processes of the studied rocks, the information attained may be very useful in new engineering applications and restoration works. According to the current results, the tested limestone specimens may be appropriate for use in areas exposed to frequent thermal and salt weathering action. However, future work should investigate the impact of weathering processes on different types of rocks for obtaining a complete evolution of the rock deterioration characteristics. Furthermore, the decay function model used here to estimate the rock durability characteristics in projected future constructions might be usefully applied on various rocks against weathering conditions for use in other studies. Therefore, the subsequent studies must select more

than one appropriate model and compare their durability changes. This might give a good impression of overall model performance and compare the results of these intermodal.

Author Contributions: Methodology, M.M.A.A. and B.G.M.; formal analysis, M.M.A.A., B.G.M. and H.W.; writing—original draft preparation, M.M.A.A., B.G.M., I.M., M.A.E. and R.A.; writing—review and editing, M.M.A.A., B.G.M. and A.M.G.; resources, S.M.E. Furthermore, R.A. supervised the whole work. All authors have read and agreed to the published version of the manuscript.

Funding: This research was funded by the Research Group Program under grant no. RGP. 2/19/43.

Institutional Review Board Statement: Not applicable.

Informed Consent Statement: Not applicable.

Data Availability Statement: Not applicable.

Acknowledgments: The authors extend their appreciation to the Deanship of Scientific Research at King Khalid University, Abha, Saudi Arabia, for funding this work.

Conflicts of Interest: The authors declare no conflict of interest.

References

- Ozcelik, Y.; Careddu, N.; Yilmazkaya, E. The effects of freeze–thaw cycles on the gloss values of polished stone surfaces. *Cold Reg. Sci. Technol.* **2012**, *82*, 49–55. [[CrossRef](#)]
- García-Del-Cura, M.A.; Benavente, D.; Martínez-Martínez, J.; Cueto, N. Sedimentary structures and physical properties of travertine and carbonate tufa building stone. *Constr. Build. Mater.* **2012**, *28*, 456–467. [[CrossRef](#)]
- Momeni, A.; Abdilor, Y.; Khanlari, G.R.; Heidari, M.; Sepahi, A.A. The effect of freeze– thaw cycles on physical and mechanical properties of granitoid hard rocks. *Bull. Eng. Geol. Environ.* **2016**, *75*, 1649–1656. [[CrossRef](#)]
- Ali, R.; Khan, I.; Ali, A.; Mohamed, A. Two new generalized iteration methods for solving absolute value equations using M-matrix. *AIMS Math.* **2022**, *7*, 8176–8187. [[CrossRef](#)]
- Zhang, Z.P.; Shao, Y.F.; Song, F. Characteristics of crack patterns controlling the retained strength of ceramics after thermal shock. *Front. Mater. Sci. China* **2010**, *4*, 251–254. [[CrossRef](#)]
- Abad, S.A.N.K.; Mohamad, E.T.; Komoo, I. Dominant weathering profiles of granite in southern Peninsular Malaysia. *Eng. Geol.* **2014**, *183*, 208–215. [[CrossRef](#)]
- Ercoli, L.; Zimbardo, M.; Nocilla, A. Rock decay phenomena and collapse processes in the Latomie del Paradiso in Syracuse (Sicily). *Eng. Geol.* **2014**, *178*, 155–165. [[CrossRef](#)]
- Abad, S.V.A.N.K.; Mohamad, E.T.; Komoo, I.; Kalatehjari, R. A typical weathering profile of granitic rock in Johor, Malaysia based on joint characterization. *Arab. J. Geosci.* **2015**, *8*, 2191–2201. [[CrossRef](#)]
- Abad, S.V.A.N.K.; Mohamad, E.T.; Komoo, I.; Kalatehjari, R. Assessment of weathering effects on rock mass structure. *J. Tekh.* **2015**, *72*, 71–75.
- Khanlari, G.; Sahamieh, R.Z.; Abdilor, Y. The effect of freeze–thaw cycles on physical and mechanical properties of Upper Red Formation sandstones, central part of Iran. *Arab. J. Geosci.* **2015**, *8*, 5991–6001. [[CrossRef](#)]
- Shushakova, V.; Edwin, R.; Fuller, E.R., Jr.; Heidelbach, F.; Mainprice, D.; Siegesmund, S. Marble decay induced by thermal strains: Simulations and experiments. *Environ. Earth. Sci.* **2013**, *69*, 1281–1297. [[CrossRef](#)]
- Andriani, G.F.; Germinario, L. Thermal decay of carbonate dimension stones: Fabric, physical and mechanical changes. *Environ. Earth. Sci.* **2014**, *72*, 2523–2539. [[CrossRef](#)]
- Ghobadi, M.H.; Babazadeh, R. Experimental studies on the effects of cyclic freezing– thawing, salt crystallization, and thermal shock on the physical and mechanical characteristics of selected sandstones. *Rock Mech. Rock Eng.* **2015**, *48*, 1001–1016. [[CrossRef](#)]
- Vazquez, P.; Shushakova, V.; Gomez-Heras, M. Influence of mineralogy on granite decay induced by temperature increase: Experimental observations and stress simulation. *Eng. Geol.* **2015**, *189*, 58–67. [[CrossRef](#)]
- Çelik, M.Y.; Sert, M. Accelerated aging laboratory tests for the evaluation of the durability of hydrophobic treated and untreated andesite with respect to salt crystallization, freezing–thawing, and thermal shock. *Bull. Eng. Geol. Environ.* **2020**, *79*, 3751–3770. [[CrossRef](#)]
- Lisci, C.; Sitzia, F.; Pires, V.; Mirão, J. Building stones durability by UVA radiation, moisture and spray accelerated weathering. *J. Build. Rehabil.* **2022**, *7*, 60. [[CrossRef](#)]
- Karakaş, A.; Morali, G.; Coruk, Ö.; Bozkurtoğlu, E. Geomechanical, durability–hygrothermal and thermal shock properties of Kocaeli Kandira stone used as building stone in historical structures. *Environ Earth Sci.* **2021**, *80*, 130. [[CrossRef](#)]
- Yavuz, A.B. Deterioration of the volcanic kerb and pavement stones in a humid environment in the city centre of Izmir, Turk. *Environ Geol.* **2006**, *51*, 211–227. [[CrossRef](#)]
- Hale, P.A.; Shakoor, A. A laboratory investigation of the effects of cyclic heating and cooling, wetting and drying, and freezing and thawing on the compressive strength of selected sandstones. *Environ. Eng. Geosci.* **2003**, *9*, 117–130. [[CrossRef](#)]

20. Sousa, L.M.O.; Suarez, L.M.; Calleja, L.; de Argandoña, V.G.R.; Rey, A.R. Influence of micro fractures and porosity on the physico-mechanical properties and weathering of ornamental granites. *Eng. Geol.* **2005**, *77*, 153–168. [[CrossRef](#)]
21. Wang, P.; Xu, J.; Liu, S.; Wang, H.; Liu, S. Static and dynamic mechanical properties of sedimentary rock after freeze-thaw or thermal shock weathering. *Eng. Geol.* **2016**, *210*, 148–157. [[CrossRef](#)]
22. Ali, R.; Pan, K.; Ali, A. Two generalized successive overrelaxation methods for solving absolute value equations. *Math. Theory Appl.* **2020**, *40*, 44–55.
23. Gokceoglu, C.; Zorlu, K.; Ceryan, S.; Nefeslioglu, H. A comparative study on indirect determination of degree of weathering of granites from some physical and strength parameters by two soft computing techniques. *Mater. Charact.* **2009**, *60*, 1317–1327. [[CrossRef](#)]
24. Mutluturk, M.; Altindag, R.; Turk, G. A decay function model for the integrity loss of rock when subjected to recurrent cycles of freezing–thawing and heating–cooling. *Int. J. Rock. Mech. Min. Sci.* **2004**, *41*, 237–244. [[CrossRef](#)]
25. Jefferson, D.P. Building stone: The geological dimension. *Q. J. Eng. Geol. Hydrol.* **1993**, *26*, 305–319. [[CrossRef](#)]
26. Doehne, E.; Price, C.A. *Stone Conservation: An Overview of Current Research*; The Getty Conservation Institute: Second edition; J Paul Getty Museum Publications: Los Angeles, CA, USA, 2010; Volume 158.
27. Benavente, D.; del Cura, M.A.G.; Fort, R.; Ordóñez, S. Thermodynamic modeling of changes induced by salt pressure crystallization in porous media of stone. *J. Cryst. Growth* **1999**, *204*, 168–178. [[CrossRef](#)]
28. Jamshidi, A.; Nikudel, M.R.; Khamehchiyan, M. Predicting the long-term durability of building stones against freeze–thaw using a decay function model. *Cold Reg. Sci. Technol.* **2013**, *92*, 29–36. [[CrossRef](#)]
29. Pitzurra, L.; Moroni, B.; Nocentini, A.; Sbaraglia, G.; Poli, G.; Bistoni, F. Microbial growth and air pollution in carbonate rock weathering. *Int. Biodeterior.* **2003**, *52*, 63–68. [[CrossRef](#)]
30. Sandrolini, F.; Franzoni, E. An operative protocol for reliable measurements of moisture in porous materials of ancient buildings. *Build. Environ.* **2006**, *41*, 1372–1380. [[CrossRef](#)]
31. Bozdağ, A. The Effect of Salt (NaCl) Crystallization on Engineering Parameters of Rocks. Ph.D. Thesis, Selcuk University, Konya, Turkey, 2013.
32. Korkanç, M. Deterioration of different stones used in historical buildings within Nigde Province, Cappadocia. *Constr. Build. Mater.* **2013**, *48*, 789–803.
33. Barone, G.; Mazzoleni, P.; Pappalardo, G.; Raneri, S. Microtextural and microstructural influence on the changes of physical and mechanical proprieties related to salts crystallization weathering in natural building stones. The example of Sabucina stone (Sicily). *Constr. Build. Mater.* **2015**, *95*, 355–365. [[CrossRef](#)]
34. Erdogan, O.; Ozvan, A. Evaluation of strength parameters and quality assessment of different lithotype levels of Edremit (Van) Travertine (Eastern Turkey). *J. Afr. Earth. Sci.* **2016**, *106*, 108–118. [[CrossRef](#)]
35. Jamshidi, A.; Nikudel, M.R.; Khamehchiyan, M. Evaluation of the durability of Gerdoee travertine after freeze–thaw cycles in fresh water and sodium sulfate solution. *Eng. Geol.* **2016**, *202*, 36–43. [[CrossRef](#)]
36. Menendez, B.; Petranova, V. Effect of mixed vs single brine composition on salt weathering in porous carbonate building stones for different environmental conditions. *Eng. Geol.* **2016**, *210*, 124–139. [[CrossRef](#)]
37. Ruffolo, S.A.; La Russa, M.F.; Ricca, M.; Belfiore, C.M.; Macchia, A.; Comite, V.; Pezzino, A.; Crisci, G.M. New insights on the consolidation of salt weathered limestone: The case study of Modica stone. *Bull. Eng. Geol. Environ.* **2017**, *76*, 11–20. [[CrossRef](#)]
38. Çelik, M.Y.; Tıgılı, R. The investigation of the water repellent chemical influence on salt crystallization in high porous building stones. *Gazi Univ. J. Eng. Arch.* **2018**, *34*, 535–552.
39. Khodabandeh, M.A.; Rozgonyi-Boissinot, N. The Effect of Salt Weathering and Water Absorption on the Ultrasonic Pulse Velocities of Highly Porous Limestone. *Period. Polytech. Civ. Eng.* **2022**, *66*, 627–639. [[CrossRef](#)]
40. Lezzerini, M.; Tomei, A.; Gallelo, G.; Aquino, A.; Pagnotta, S. The Crystallization Effect of Sodium Sulfate on Some Italian Marbles, Calcarenites and Sandstones. *Heritage* **2022**, *5*, 1449–1461. [[CrossRef](#)]
41. Çelik, M.Y.; İbrahimoglu, A. Characterization of travertine stones from Turkey and assessment of their durability to salt crystallization. *J. Build. Eng.* **2021**, *43*, 102592. [[CrossRef](#)]
42. Oguchi, C.T.; Yu, S. A review of theoretical salt weathering studies for stone heritage. *Prog. Earth Planet. Sci.* **2021**, *8*, 32. [[CrossRef](#)]
43. Angeli, M.; Heber, R.; Menendez, B.; David, C.; Bigas, J.-P. Influence of temperature and salt concentration on the salt weathering of a sedimentary stone with sodium sulphate. *Eng. Geol.* **2010**, *115*, 193–199. [[CrossRef](#)]
44. Cultrone, G.; Luque, A.; Sebastián, E. Petrophysical and durability tests on sedimentary stones to evaluate their quality as building materials. *Q. J. Eng. Geol. Hydrog.* **2012**, *45*, 415–422. [[CrossRef](#)]
45. Vázquez, P.; Alonso, F.; Carrizo, L.; Molina, E.; Cultrone, G.; Blanco, M.; Zamora, I. Evaluation of the petrophysical properties of sedimentary building stones in order to establish quality criteria. *Constr. Build. Mater.* **2013**, *41*, 868–878. [[CrossRef](#)]
46. Yavuz, A.B.; Topal, T. Thermal and salt crystallization effects on marble deterioration: Examples from Western Anatolia, Turkey. *Eng. Geol.* **2007**, *90*, 30–40. [[CrossRef](#)]
47. Benavente, D.; Cueto, N.; Martínez-Martínez, J.; Del Cura, M.A.G.; Cañaveras, J.C. The influence of petrophysical properties on the salt weathering of porous building rocks. *Environ. Geol.* **2007**, *52*, 197–206. [[CrossRef](#)]
48. Yavuz, A.B.; Kaputoglu, S.A.; Çolak, M.; Tanyu, B.F. Durability assessments of rare green andesites widely used as building stones in Buca (Izmir), Turkey. *Environ. Earth Sci.* **2017**, *76*, 211. [[CrossRef](#)]
49. Ruedrich, J.; Siegesmund, S. Salt and ice crystallisation in porous sandstones. *Environ. Geol.* **2007**, *52*, 225–249. [[CrossRef](#)]

50. Yavuz, H. Effect of freeze–thaw and thermal shock weathering on the physical and mechanical properties of an andesite stone. *Bull. Eng. Geol. Environ.* **2011**, *70*, 187–192. [[CrossRef](#)]
51. Liu, Q.S.; Huang, S.B.; Kang, Y.S.; Liu, X.W. A prediction model for uniaxial compressive strength of deteriorated rocks due to freeze–thaw. *Cold Reg. Sci. Technol.* **2015**, *120*, 96–107. [[CrossRef](#)]
52. *TS EN 1936*; Natural Stone Test Methods–Determination of Real Density and Apparent Density and of Total and Open Porosity. Turkish Standards Institute: Ankara, Turkey, 2010; p. 10.
53. *TS EN 13755*; Natural Stone Test Methods–Determination of Water Absorption at Atmospheric Pressure. Turkish Standards Institute: Ankara, Turkey, 2009; p. 10.
54. ISRM. *Rock Characterization, Testing, and Monitoring*; ISRM Suggested Methods, Pergamon Press: Oxford, UK, 1981.
55. *TS EN 1926*; Natural Stone Test Methods–Determination of Uniaxial Compressive Strength. Turkish Standards Institute: Ankara, Turkey, 2007; p. 19.
56. ISRM. Suggested methods for determining tensile strength of rock materials. *Int. J. Rock. Mech. Min. Sci. Geomech. Abstr.* **1978**, *15*, 99–103. [[CrossRef](#)]
57. Aydin, A. ISRM suggested method for determination of the Schmidt hammer rebound hardness: Revised version. In *The ISRM Suggested Methods for Rock Characterization, Testing and Monitoring: 2007–2014 SE-2*; Ulusay, R., Ed.; Springer: Berlin/Heidelberg, Germany, 2015; pp. 25–33.
58. Martínez-Martínez, J.; Benavente, D.; García-del-Cura, M.A. Spatial attenuation: The most sensitive ultrasonic parameter for detecting petrographic features and decay processes in carbonate rocks. *Eng. Geol.* **2011**, *119*, 84–95. [[CrossRef](#)]
59. *Turkish Standards Institute*; Natural Stone Test Methods—Determination of Resistance to Ageing by Thermal Shock. Institute of Turkish Standards: Ankara, Turkey, 2004; p. 3.
60. Rothert, E.; Eggers, T.; Cassar, J.; Ruedrich, J.; Fitzner, B.; Siegesmund, S. Stone properties and weathering induced by salt crystallization of Maltese Globigerina Limestone. *Geol. Soc. Lond. Spec. Publ.* **2007**, *271*, 189. [[CrossRef](#)]
61. Ruedrich, J.; Kirchner, D.; Siegesmund, S. Physical weathering of building stones induced by freeze–thaw action: A laboratory long term study. *Environ. Earth. Sci.* **2011**, *63*, 1573–1586. [[CrossRef](#)]
62. Benavente, D.; Pla, C.; Cueto, N.; Galvañ, S.; Martínez-Martínez, J.; García-Del-Cura, M.; Ordóñez, S. Predicting water permeability in sedimentary rocks from capillary imbibition and pore structure. *Eng. Geol.* **2015**, *195*, 301–311. [[CrossRef](#)]
63. Akin, A.; Ozsan, A. Evaluation of the long-term durability of yellow travertine using accelerated weathering tests. *Bull. Eng. Geol. Environ.* **2011**, *70*, 101–114. [[CrossRef](#)]
64. Tuğrul, A. The effect of weathering on the pore geometry and compressive strength of selected rock types from Turkey. *Eng. Geol.* **2004**, *75*, 215–227. [[CrossRef](#)]
65. Diamantis, K.; Gartzos, E.; Migiros, G. Study on uniaxial compressive strength, point load strength index, dynamic and physical properties of serpentinites from Central Greece: Test results and empirical relations. *Eng. Geol.* **2009**, *108*, 199–207. [[CrossRef](#)]
66. Ahmad, A.; Pamplona, M.; Simon, S. Ultrasonic testing for the investigation and characterization of stone—A non-destructive and transportable tool. *Stud. Conserv.* **2009**, *54*, 43–53. [[CrossRef](#)]
67. La Iglesia, A.; González, V.; López-Acevedo, V.; Viedma, C. Salt crystallization in porous construction materials. I. Estimation of crystallization pressure. *J. Cryst. Growth* **1997**, *177*, 111–118. [[CrossRef](#)]
68. Johnson, R.A.; Wichern, D.W. *Applied Multivariate Statistical Analysis*, 5th ed.; Prentice-Hall: Englewood Cliffs, NJ, USA, 1999.
69. Eren, O.; Bahali, M. Some engineering properties of natural building cut stones of Cyprus. *Constr. Build. Mater.* **2005**, *19*, 213–222. [[CrossRef](#)]